Title

Motor network gamma oscillations in chronic home recordings predict dyskinesia in Parkinsons disease.

Journal

Brain, 147(6)

Authors

Olaru, Maria
Cernera, Stephanie
Hahn, Amelia
et al.

Publication Date

2024-06-03

DOI

10.1093/brain/awae004

Peer reviewed

BRAIN
ORIGINAL ARTICLE

Motor network gamma oscillations in chronic home recordings predict dyskinesia in Parkinson's disease

Maria Olaru,[1,2] Stephanie Cernera,[1,2] Amelia Hahn,[1,2] Thomas A. Wozny,[1,2] Juan Anso,[1,2] Coralie de Hemptinne,[3] Simon Little,[2] Wolf-Julian Neumann,[4] Reza Abbasi-Asl[2,5] and Philip A. Starr[1,2]

In Parkinson's disease, imbalances between 'antikinetic' and 'prokinetic' patterns of neuronal oscillatory activity are related to motor dysfunction. Invasive brain recordings from the motor network have suggested that medical or surgical therapy can promote a prokinetic state by inducing narrowband gamma rhythms (65–90 Hz). Excessive narrowband gamma in the motor cortex promotes dyskinesia in rodent models, but the relationship between narrowband gamma and dyskinesia in humans has not been well established.

To assess this relationship, we used a sensing-enabled deep brain stimulator system, attached to both motor cortex and basal ganglia (subthalamic or pallidal) leads, paired with wearable devices that continuously tracked motor signs in the contralateral upper limbs. We recorded 984 h of multisite field potentials in 30 hemispheres of 16 subjects with Parkinson's disease (2/16 female, mean age 57 ± 12 years) while at home on usual antiparkinsonian medications. Recordings were done 2–4 weeks after implantation, prior to starting therapeutic stimulation.

Narrowband gamma was detected in the precentral gyrus, subthalamic nucleus or both structures on at least one side of 92% of subjects with a clinical history of dyskinesia. Narrowband gamma was not detected in the globus pallidus. Narrowband gamma spectral power in both structures co-fluctuated similarly with contralateral wearable dyskinesia scores (mean correlation coefficient of $\rho = 0.48$ with a range of 0.12–0.82 for cortex, $\rho = 0.53$ with a range of 0.5–0.77 for subthalamic nucleus). Stratification analysis showed the correlations were not driven by outlier values, and narrowband gamma could distinguish 'on' periods with dyskinesia from 'on' periods without dyskinesia. Time lag comparisons confirmed that gamma oscillations herald dyskinesia onset without a time lag in either structure when using 2-min epochs. A linear model incorporating the three oscillatory bands (beta, theta/alpha and narrowband gamma) increased the predictive power of dyskinesia for several subject hemispheres. We further identified spectrally distinct oscillations in the low gamma range (40–60 Hz) in three subjects, but the relationship of low gamma oscillations to dyskinesia was variable.

Our findings support the hypothesis that excessive oscillatory activity at 65–90 Hz in the motor network tracks with dyskinesia similarly across both structures, without a detectable time lag. This rhythm may serve as a promising control signal for closed-loop deep brain stimulation using either cortical or subthalamic detection.

1 Department of Neurological Surgery, University of California San Francisco, San Francisco, CA 94143, USA
2 Weill Institute for Neurosciences, University of California San Francisco, San Francisco, CA 94158, USA
3 Department of Neurology, University of Florida Gainesville, Gainesville, FL 32611, USA
4 Movement Disorder and Neuromodulation Unit, Department of Neurology, Charité – Universitätsmedizin Berlin, corporate member of Freie Universität Berlin and Humboldt-Universität zu Berlin, Berlin 10117, Germany
5 Department of Neurology, University of California San Francisco, San Francisco, CA 94143, USA

Received August 09, 2023. Revised December 17, 2023. Accepted December 21, 2023. Advance access publication January 9, 2024

Correspondence to: Maria Olaru
Department of Neurological Surgery
University of California San Francisco
513 Parnassus Ave, HSE-823
San Francisco, CA 94143-0350, USA
E-mail: maria.olaru@ucsf.edu

Keywords: deep brain stimulation; neurological movement disorders; physiological biomarkers; physiopathology; wearable electronic devices; wireless technology

Introduction

Much has been learned about the physiological basis for Parkinsonian motor signs by recording local field potentials from deep brain stimulator leads implanted in basal ganglia nuclei. Early work used externalized leads in subjects at rest in a perioperative setting.[1] A seminal early observation using externalized leads was that therapeutic levodopa suppressed subthalamic nucleus beta band (13–30 Hz) oscillatory activity while promoting gamma band activity at 65–90 Hz, often referred to as 'narrowband gamma' or as 'finely-tuned gamma'.[2] This led to the hypothesis that alleviating bradykinesia requires rebalancing basal ganglia 'antikinetic' beta oscillations with 'prokinetic' higher frequency oscillations. This model suggests an excess of the 'prokinetic' narrowband gamma rhythm could lead to hyperkinetic states such as dyskinesia. However, this link has been difficult to demonstrate with short perioperative recordings from externalized leads.

In rodent models of Parkinson's disease treated chronically with levodopa, phenomenologically identical 65–90 Hz narrowband gamma oscillations have been recorded from the motor cortex, where they are linked to dyskinesia.[3-5] Recently, narrowband gamma has been observed in the motor cortex of subjects with Parkinson's disease in the ON-medication state with first-generation[6] and second-generation[7] sensing-enabled deep brain stimulation (DBS) devices connected to subdural cortical leads. In humans with Parkinson's disease, Swann *et al.*[6] suggested a relationship between cortical narrowband gamma and dyskinesia in two subjects from multiple brief recordings at home in dyskinetic and non-dyskinetic states. However, those findings were based on short recordings (30-s to 5-min duration) and subject self-ratings for dyskinesia. The remaining questions include: (i) whether narrowband gamma spectral power in the motor network scales with the severity of dyskinesias; (ii) the temporal relationship between variations in narrowband gamma and variations in dyskinesia; (iii) the relative value of cortical versus basal ganglia narrowband gamma as markers of dyskinesia; and (iv) the contribution of the other frequencies, such as beta and theta, as covariate predictors of dyskinesia.[8]

To address these questions, we utilized an investigational second-generation sensing-enabled pulse generator capable of performing four-channel recordings continuously at home.[7] Prior to initiating therapeutic basal ganglia stimulation, we recorded 984 h of cortical and basal ganglia field potentials in 30 hemispheres of 16 subjects with Parkinson's disease, with 608 h recorded while continuously measuring dyskinesia using wearable sensors. We collected recordings in naturalistic settings while subjects were awake, performing normal activities of daily living and on their usual schedule of antiparkinsonian medications. We found fluctuations in narrowband gamma spectral power in both the motor cortex and subthalamic nucleus correlate to fluctuations in continuous metrics of dyskinesia with minimal time lag.

Materials and methods

Subject selection and assessment

The institutional review board approved the study protocol and we registered the study on clinicaltrials.gov (NCT03582891) under a physician-sponsored investigational device exemption for Medtronic's Summit RC+S (G180097/R003). We collected data from 16 subjects with Parkinson's disease implanted with an investigational bidirectional neural interface, Summit RC+S (Medtronic Inc.), designed for chronic sensing of field potentials during activities of daily living.[9] We attached depth leads to the device in either the subthalamic nucleus (11 subjects) or globus pallidus (five subjects) and paddle-type leads placed subdurally over precentral and postcentral gyri.[7] Data from the first five subjects have been published previously in an unrelated analysis that did not specifically address dyskinesias.[7] We recruited participants from the movement disorders surgery clinic at the University of California San Francisco in accordance with the Declaration of Helsinki. Inclusion criteria were a diagnosis of idiopathic Parkinson's disease by a movement disorders neurologist and standard clinical indications for subthalamic nucleus or globus pallidus deep brain stimulation.[10,11] Exclusion criteria were significant cognitive impairment as determined by a Montreal Cognitive Assessment score of 20 or lower or an untreated mood disorder as evaluated by a neuropsychologist. A movement disorders specialist evaluated baseline motor function prior to implantation using the Movement Disorder Society revision of the Unified Parkinson's Disease Rating Scale part III (UPDRS III) in the OFF- and ON-medication states. The OFF-medication state is 12 h after withdrawal of antiparkinsonian medication, and the ON-medication state is 30–45 min after a supratherapeutic dose of carbidopa-levodopa. We characterized the baseline severity of dyskinesia in daily life using UPDRS IVa 4.1 (time spent with dyskinesia). We determined whether motor signs in one hemibody were more severe than the other using UPDRS III OFF-medication scores for rigidity, bradykinesia and tremor in each limb.

Surgical implantation

We implanted all subjects with quadripolar cylindrical leads in either the subthalamic nucleus (Medtronic 3389 lead) or globus pallidus (Medtronic 3387 lead), consisting of 1.5 mm or 3 mm intercontact spacing, respectively, and quadripolar paddle-type cortical leads (10 mm intercontact spacing) using methods previously described (Fig. 1A).[7,12] The surgeon placed cortical leads along

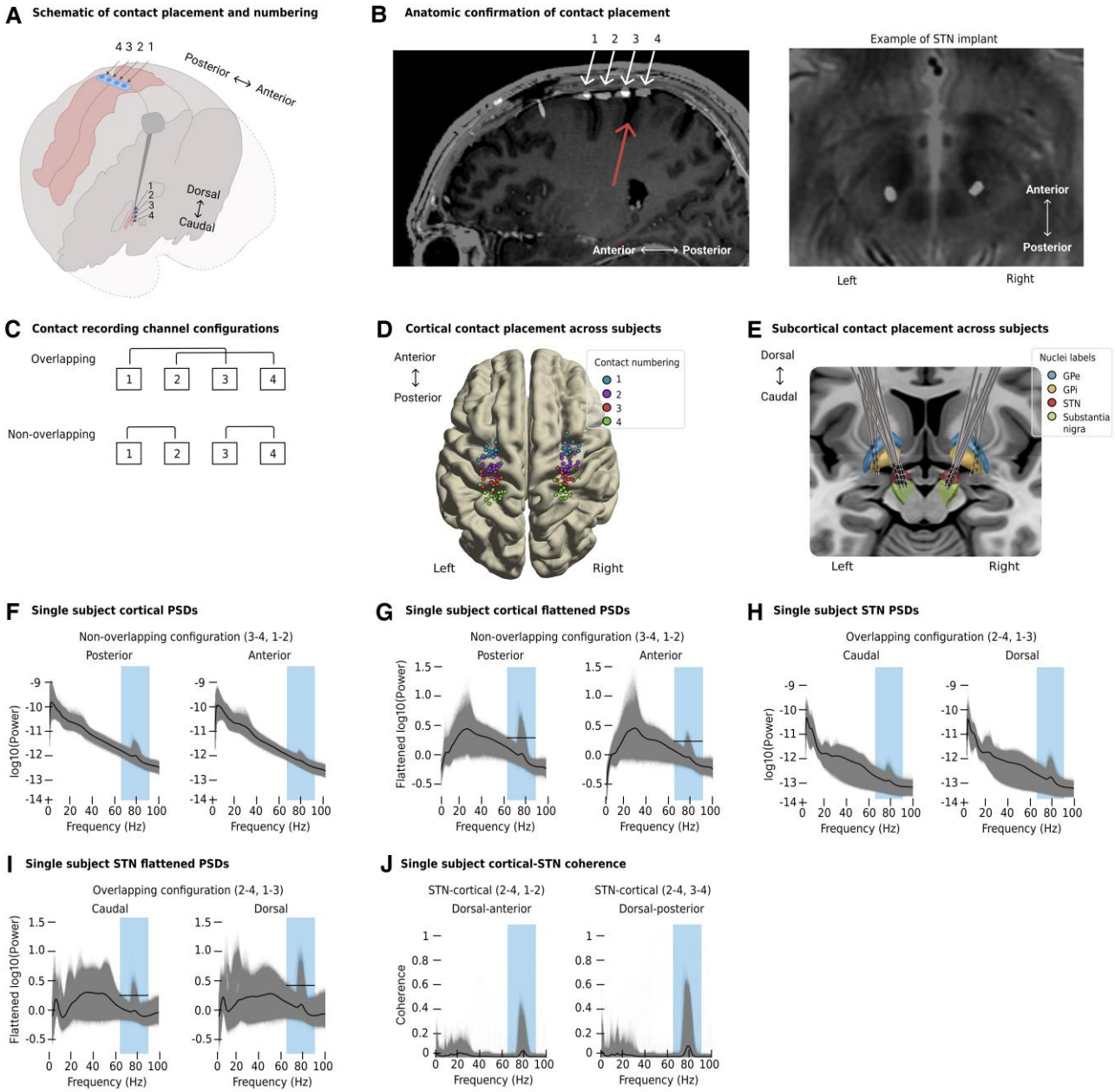

Figure 1 Anatomic localization of recording contacts and data processing method. (**A**) A schematic of the cortical paddle and subcortical depth lead locations (hardware shown on only one side for clarity), where each contact is labelled 1–4 (anterior-posterior for the cortical paddle, dorsal-caudal for the subcortical depth lead). (**B**) An example of cortical (*left*) and subthalamic (*right*) leads in an individual subject (Subject 1) on a parasagittal MRI (*left*) and an axial MRI at the level of the dorsal subthalamic nucleus (STN) (*right*). The largest arrow (red) marks the central sulcus. (**C**) *Top*: The overlapping bipolar recording configuration using contact pairs 1–3 and 2–4. For cortical recordings, this was the configuration used to record from Subjects 1–5. For subcortical recordings, this was the configuration used to record from subthalamic-implanted subjects. *Bottom*: The non-overlapping bipolar recording configuration using contact pairs 1–2 and 3–4. For cortical recordings, this was the configuration used to record from Subjects 6–16. For subcortical recordings, this was the configuration used to record from pallidal-implanted subjects. (**D**) Cortical contact placement across subjects represented on a template brain. (**E**) Location of all subcortical depth leads represented on a template brain. (**F**) Single subject example (Subject 4, right hemisphere) of overlaid power spectral densities (PSDs) from the posterior (*left*) and anterior (*right*) recording configurations of the cortical paddle (log-scaled) during everyday life at home. Each power spectral density line (grey) was derived from a 2-min recording. The average power spectra is overlaid as the black line. The rectangle spanning 65–90 Hz (blue) denotes the signal frequencies that characterize narrowband gamma. (**G**) Overlaid power spectral densities from **F** after removing aperiodic activity using the Fitting Oscillations and One-Over-F (FOOOF) algorithm.[13] The flattened average power spectra is overlaid as the black line. The horizontal line (black) in the rectangle is the power threshold used to detect the peak narrowband gamma frequency. (**H**) Example of overlaid power spectral densities from the caudal (*left*) and dorsal (*right*) recording configurations of the subthalamic lead using the same format as in **F**. (**I**) Overlaid power spectral densities from **H** after removing aperiodic activity using FOOOF, similar to **G**. (**J**) The coherence between the channel with the maximum integrated gamma score (dorsal) and the two channels (anterior and posterior) from the remaining implant site (cortical). GPe = globus pallidus external; GPi = globus pallidus internal; NBG = narrowband gamma.

a parasagittal trajectory such that either two or three contacts were anterior to the central sulcus, 2–4 cm from the midline. We confirmed electrode localization intraoperatively using cone beam CT (Medtronic O-arm)[14] fused to preoperative MRI (Fig. 1B). For each implanted hemisphere, we connected brain leads to a Medtronic Summit RC+S interface (model B35300R) in the ipsilateral pectoral area via 60 cm lead extenders (model 37087). We covered the connection between the lead extender and implantable pulse generator (Summit RC+S) with medical adhesive to reduce leakage of the ECG signal into neural recordings.[15]

Electrodes could then be configured into several types of bipolar recording configurations (Fig. 1C). Precise anatomic electrode localization was refined *post hoc* using established image analysis pipelines for deep brain stimulation[16] and cortical electrodes.[17] Briefly, we coregistered post-implantation high-resolution CT images using a rigid, linear affine transformation and resliced into a preoperative T1-weighted 3 T MRI.[18] We verified placement by visual inspection and, when necessary, implemented an additional brain shift correction to refine subcortical anatomy coregistration.[19] Then, we localized electrodes to CT artefacts. Lastly, we applied an additional surface projection correction[20] to localize cortical leads to the MRI-rendered pial surface.[18] For group analyses, we normalized electrode locations into Montreal Neurological Institute space[18] and visualized either on the FreeSurfer average cortical surface[21] (Fig. 1D) or a standardized Parkinson's disease-specific subcortical atlas (Fig. 1E).[22]

Signal recording

Neural

We analysed intracranial sensorimotor cortical and basal ganglia field potentials from subjects with chronically implanted cortical paddles and depth leads in the home environment while engaging in activities of daily living. Recordings were completed more than 1 week after implantation, before initiating therapeutic deep brain stimulation 1 month after implantation, and for recording durations of at least 8 h per hemisphere. For cortical recordings in Subjects 1–5, we configured overlapping bipolar recording channels (contacts 1–3 and 2–4) and configured all subsequent subjects with non-overlapping bipolar recording channels (contacts 1–2 and 3–4). For the non-overlapping recording channels from the cortical site, the recording configuration from contacts 1–2 sampled the precentral gyrus, while the recording configuration from contacts 3–4 sampled the postcentral gyrus. For depth leads, we configured subthalamic-implanted subjects with overlapping recording channels and pallidal-implanted subjects with non-overlapping recording channels (Fig. 1C). Subjects streamed neural data from the Summit RC+S interface to a Microsoft Windows tablet using a custom-made graphical user interface on the device's application program made available by Medtronic Inc. (all software is compliant with the US Food and Drug Administration code CFR 820.30 and accessible at https://openmind-consortium.github.io).[7] Subjects with bilateral implants streamed data from both hemispheres simultaneously. Each RC+S streamed potentials in the time domain from two channels per cortical paddle at a sampling rate of 250 or 500 Hz. The device enables up to 30 h of continuous recording prior to recharging.

Wearable

Subjects streamed neural data at home while wearing Global Kinetics Pty Ltd. Personal KinetiGraph® (PKG®) monitors[23,24] on both wrists during normal daily activities and while on their preoperative dose of antiparkinsonian medication (Table 1). This wearable device provides continuous tremor, bradykinesia and dyskinesia scores in 2-min intervals using a three-axis accelerometer and a proprietary, validated commercial algorithm.[25] Each wearable device records data for a maximum of 9 days before requiring an additional charge. We removed outliers from the wearable data by excluding all values more than 4 SD from each subject's mean score, a standard practice for large datasets.[26] While PKG® scores have been clinically validated with respect to UPDRS ratings,[27] we performed additional validation within our data, showing a correlation of averaged wearable dyskinesia scores and UPDRS IV ratings of $\rho = 0.51$ ($P = 0.004$; Supplementary Fig. 2A). The relationship between averaged wearable dyskinesia scores and UPDRS IV ratings suggests that these scores can

Table 1 Subject demographics

Pt	Symptoms (years)	UPDRS (OFF)	UPDRS IV	Levodopa (mg)	Age (years)	Gender	MOCA	UPDRS tremor L	UPDRS tremor R	UPDRS (OFF-ON)	Implant site	Implant side
1	7	49	4	1425	54	M	26	2	0	0.9	STN	Bilateral
2	19	45	1	955	63	M	30	3	4	0.51	STN	Bilateral
3	12	61	2	1550	28	F	27	12	9	0.73	STN	Bilateral
4	4	41	1	1314	40	M	30	6	3	0.65	STN	Bilateral
5	12	44	2	2100	58	M	27	0	0	0.75	STN	Bilateral
6	10	39	2	1755	48	M	27	6	14	0.59	GP	Bilateral
7	13	89	0	1083	64	F	27	9	11	0.53	GP	Bilateral
8	7	29	2	1525	71	M	26	0	4	0.58	STN	Bilateral
9	10	34	2	800	58	M	28	4	10	0.73	STN	Bilateral
10	4	31	0	1580	65	M	26	7	4	0.51	GP	Unilateral
11	6	35	0	570	61	M	27	7	7	0.67	STN	Bilateral
12	12	32	1	920	45	M	26	3	3	0.84	STN	Bilateral
13	7	49	2	2031	67	M	27	1	1	0.76	STN	Bilateral
14	8	49	0	1213	51	M	27	14	3	0.61	GP	Bilateral
15	13	31	1	1036	73	M	28	4	4	0.67	STN	Bilateral
16	9	66	1	900	66	M	29	12	11	0.64	GP	Unilateral

The Unified Parkinson's Disease Rating Scale (UPDRS) tremor L/R ratings are derived from questions from the contralateral UPDRS III 15–17 in the OFF-medication state. The UPDRS dyskinesia rating is from question UPDRS IVa 4.1. The UPDRS OFF-ON score is the per cent change in overall motor symptoms (UPDRS III) between clinically defined OFF-medication and ON-medication states. The OFF-medication state is defined as 12 h after withdrawal of antiparkinsonian medication, and the ON-medication state is defined as 30–45 min after a supratherapeutic dose of carbidopa-levodopa. F = female; GP = globus pallidus; M = male; MOCA = Montreal Cognitive Assessment; OFF = OFF medication; ON = ON medication; Pt = Subject; STN = subthalamic nucleus.

approximate involuntary hyperkinetic movement, versus primarily normal voluntary movement.

Signal processing

Neural

We first derived timestamps for field potentials and reformatted cortical and basal ganglia field potentials from the RC+S system using a validated open-source toolbox in MATLAB R2019b.[28] For subjects with recordings containing multiple channel configurations, we processed the channel configuration with the longest recorded data to increase the dyskinetic fluctuations during recordings (for subject-specific channel configurations, see Fig. 1C, Signal Recording–Neural). Then, we downsampled the potentials to 250 Hz and calculated the power spectral density for each channel in non-overlapping 2-min intervals using the Welch method (Python 3.8.3 SciPy package).[29] We used non-overlapping Hann windows of 256 data-points per fast Fourier transform for the cortical (Fig. 1F) and subcortical (Fig. 1H) channels.

Power spectra from all 2-min epochs were overlaid for each channel and processed to identify narrow band peaks within a frequency band of interest (65–90 Hz for narrowband gamma). Given the temporal variability of peak presence and dyskinesia in this large dataset, we employed three steps to increase the signal-to-noise ratio and focus on epochs with high oscillatory activity. First, we flattened the spectra by removing the aperiodic component from all 2-min epochs using the Fitting Oscillations and One-Over-F (FOOOF) algorithm.[13] Second, we defined the peak frequency oscillation as the most commonly occurring frequency (within the frequency band of interest) with maximum spectral power (at least 2 SD above the mean at 65 Hz) across all epochs (Supplementary Fig. 1A). A single peak frequency was used for all data epochs from a given recording site and hemisphere but was individualized across hemispheres, recording sites within a hemisphere, and frequency bands within a recording site. Additional analyses regarding the variability of peak gamma frequency across epochs within a subject hemisphere can be found in the intra-subject hemisphere variability section of the Supplementary material. We used the 65 Hz frequency as a baseline because even after removing aperiodic activity, lower frequency activity may exhibit higher power values. Third, we defined epochs as containing oscillatory signals if the peak frequency power was at least 2 SD above the mean peak frequency power. We included all visually detectable FOOOF peaks in the unflattened overlaid power spectra (when identifying narrow band peaks using the low-gamma frequency band, some FOOOF peaks detected were broadband gamma, not narrowband peaks).

To generate summary statistics for the oscillatory signal, we defined an integrated narrowband gamma score that considers not only the power but also the temporal duration of the oscillation. To do this, we averaged the power spectral densities for all epochs that met the criteria for having an oscillatory peak and multiplied this by the percentage of the recording time during which the oscillation was present. For each electrode (two channels per electrode), we defined the dominant channel as having the largest integrated narrowband gamma score. The dominant channel was defined independently for each spectral power band. For comparisons of spectral power to wearable scores, we used the peak frequency of the dominant channel as determined from flattened spectra (as in Fig. 1G and I), with the amplitude of that frequency in the unflattened, log-scaled power spectra (as in Fig. 1F and H) for each subject hemisphere, since the latter is more relevant for evaluation of these signals in adaptive deep brain stimulation.

Lastly, we characterized narrowband gamma coherence using Python's 'SciPy' package[29] between the recording site with the maximal integrated narrowband gamma score and the two channels from the remaining recording site (Fig. 1J). Then, we determined the dominant paired channels as those with the largest integrated narrowband gamma score using the above methods. We also visually observed distinct low gamma spectral peaks (40–60 Hz) in three subjects and thus employed these methods to characterize low gamma cortical and subcortical 6oscillations.

Wearable

Wearable dyskinesia and tremor scores were labelled such that higher scores indicated more severe motor signs. We transformed wearable bradykinesia scores from negative to positive values, such that higher scores also indicated more severe motor signs. Next, we removed data from periods of sleep using immobility as a surrogate marker, defined as ≥2 min with a bradykinesia score >80.[30]

Time alignment

To align neural and wearable data, we set the wearable devices to computer clock time as determined by the network time protocol. We used computer clock time stamps from the neural data stream. To verify synchronization, we compared the root-mean-square voltage of the built-in internal accelerometer of the RC+S to the wearable accelerometer across synchronized time stamps in a subset of five subjects.[7]

Statistics

We used modules in Python for our statistical analyses. We measured time series correlations using Spearman's statistics as the default statistic, as this measure is robust to outliers. For correlations across aggregate/non-continuous measures, we used Pearson's statistics in the SciPy statistics module.[29] To visually compare time series data between neural and wearable datasets of a subject hemisphere and the contralateral wrist, we rescaled each signal using minimum-maximum normalization from the 'sklearn' module[31] onto a common scale. Normalization is standard practice for variables with large differences in scale. It does not impact statistical tests that do not rely on distance measures between examples (such as Spearman or Pearson statistics).[26] For linear regression analysis, we used the sklearn package. We split data into an 80/20 ratio of training and testing subsets. Using the training subset, we trained a linear regression model and calculated the correlation coefficient (r) between the predicted and actual dependent variable from the testing subset. For cross-validation, we regenerated the data split ratio five times across non-overlapping epochs of the data. Then, we averaged all statistics across each split.

We corrected all P-values for multiple comparisons within each subject hemisphere using false discovery rate correction in the 'statsmodel' statistics 'multitest' module.[32] We assessed effect size using Cohen's d statistic with the built-in statistics module. We compared distributions of gamma-wearable correlations across neural sites and wearable motor signs using one-way ANOVA tests. We assessed normality in each distribution with the Shapiro normality test from the SciPy statistics module. We used t-tests to compare distributions that did meet the criteria for normality and the Mann–Whitney U-test for distributions that did not. We averaged the integrated gamma scores across hemispheres for clinical measures available at the subject but not the hemibody level. To determine the total hours recorded, we summed the hemisphere with the maximal recorded configuration of each subject.

Outlier values may influence standard linear correlation techniques. Thus, in addition to using Spearman's coefficient, we used

another stratification method, described later, to assess the relationship between narrowband gamma activity and dyskinesia within individual subjects. We transformed the wearable dyskinesia numerical output to have discrete ordinal labels.[26] We binned the dyskinesia scores from bins 0–3 in an exponential manner, such that each consecutive bin contains half the amount of values as the previous bin, to mimic the duration of time subjects experience dyskinesia theoretically. Bin 4 contains all the remaining values. The ordinal bin with a label of 0 corresponds to the lowest 50th percentile of dyskinesia scores, with each consecutive label containing the remaining lowest 50th percentile of scores such that bin 0 contains percentiles 0–50; bin 1 contains percentiles 51–75; bin 2 contains percentiles 76–87.5; bin 3 contains percentiles 87.6–93.75; and bin 4 contains percentiles 93.76–100. We compared differences in narrowband gamma power for each subject hemisphere across paired sets of binned wearable dyskinesia scores (0–1, 1–2, 2–3, 3–4) with *t*-tests in the SciPy statistics module.[29] We excluded subjects without a clinical history of dyskinesia using UPDRS IVa scores in data visualization for Figs 3–5 ($n = 4$).

Results

Subject characteristics

We implanted 30 hemispheres from 16 subjects with Parkinson's disease with cortical and basal ganglia leads (2/16 female, mean age at surgery 57 ± 12 years). Subject demographics are in Table 1. Twelve subjects had a clinical history of dyskinesia (UPDRS IVa dyskinesia score >0), 10 of whom had implants in the subthalamic nucleus. In the OFF-medication state, 15 subjects had mild to moderate tremor scores in at least one limb (UPDRS III 15–17), and all subjects had non-zero bradykinesia scores in all limbs (UPDRS III 4–9, 14, recorded in the OFF-medication state).

Narrowband gamma oscillations across subjects: characteristics and relationship to the clinical history of dyskinesia

We defined the presence of narrowband gamma at the hemisphere level by inspecting each 2-min flattened power spectral density epoch for spectral power greater than 2 SD above the 1/*f* background (see the 'Material and methods' section; Fig. 1G and I). Cortical narrowband gamma was present in 20/30 hemispheres (13/16 subjects), and subthalamic narrowband gamma was present in 13/22 hemispheres and one or both hemispheres of 8/11 subjects (Table 2). None of the five subjects with pallidal depth leads met the criteria for subcortical narrowband gamma; thus all subsequent analyses of subcortical activity used only subthalamic recordings.

Frequency distribution and anatomic localization

We visualized the distribution of cortical and subthalamic narrowband gamma peak frequencies between 65 Hz and 90 Hz (Fig. 2A). Subject hemispheres with cortical and subthalamic oscillations ($n = 11$) tended to have similar peak frequencies across sites, with a median frequency peak absolute difference of 1 Hz between the cortical and subthalamic sites (Fig. 2B).

All cortical electrode arrays spanned the precentral gyrus, with at least one contact over the postcentral gyrus. For later subjects in the protocol, the central sulcus was used as the midpoint of cortical quadripolar arrays. For these subjects, we recorded cortical field potentials using non-overlapping bipolar montages (Fig. 1C) to distinguish oscillatory activity in the precentral versus postcentral gyrus. Narrowband gamma localized to the precentral gyrus in all 13 hemispheres with narrowband gamma and non-overlapping bipolar montages.

Relation to clinical history of dyskinesia

Here, we report subject-level metrics because clinical dyskinesia scores were available at the level of the subject but not the hemisphere. We defined subjects as having narrowband gamma if the signal was present in one or both hemispheres. Of the subjects who met the criteria for dyskinesia preoperatively (UPDRS IVa score >0), cortical narrowband gamma was present in 17/23 hemispheres ($n = 11/12$ subjects) and subthalamic narrowband gamma was present in 13/20 hemispheres ($n = 8/10$ subjects). Of the subjects who did not meet the clinical criteria for dyskinesia, cortical narrowband gamma was present in $n = 2/4$ subjects. Subthalamic narrowband gamma was absent

Table 2 Presence and localization of narrowband gamma across study subjects

Pt	Implant site	UPDRS IV	Left cortical		Right cortical		Left subcortical		Right subcortical	
			NBG	Correlation	NBG	Correlation	NBG	Correlation	NBG	Correlation
1	STN	4	True	True	True	True	True	True	True	True
2	STN	1	False	False	True	True	False	False	True	True
3	STN	2	False	False	False	False	False	False	False	False
4	STN	1	True	True	True	True	True	True	True	True
5	STN	2	True	False	True	True	False	False	True	True
8	STN	2	False	False	True	True	False	False	False	False
9	STN	2	True	True	True	True	True	True	True	True
11	STN	0	False	False	True	False	False	False	False	False
12	STN	1	True	True	False	False	True	True	False	False
13	STN	2	True	True	True	False	True	True	True	False
15	STN	1	True	True	False	False	True	True	True	True
6	GP	2	True	True	True	True	False	True	False	False
7	GP	0	True	True	True	True	False	False	False	False
10	GP	0	False	False	NA	NA	False	False	NA	NA
14	GP	0	False	False	False	False	False	False	False	False
16	GP	1	True	True	NA	NA	False	False	NA	NA

The presence of narrowband gamma (True or False) and significant correlations between narrowband gamma and dyskinesia (True or False) are shown across sites for all subject hemispheres. GP = globus pallidus; NA = not applicable; NBG = narrowband gamma; Pt = Subject; STN = subthalamic nucleus.

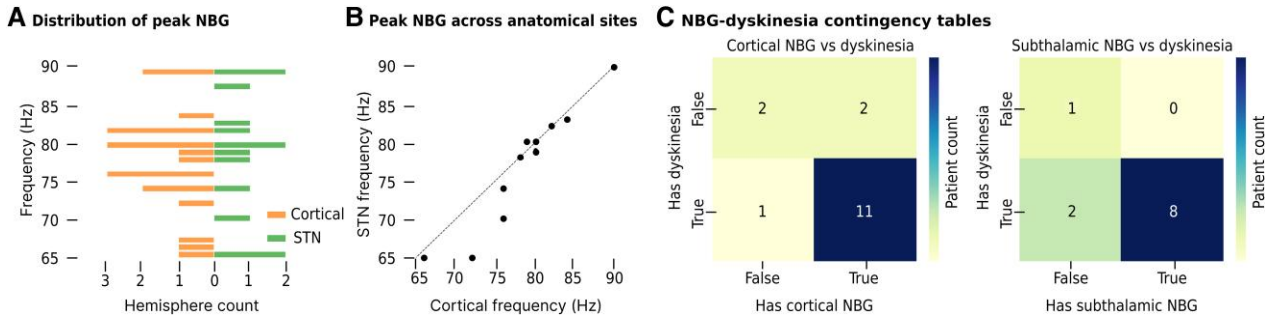

Figure 2 Narrowband gamma oscillations across subjects: frequency distribution and relation to clinical history of dyskinesia. (**A**) The distribution of peak narrowband gamma (NBG) frequencies in cortical (orange, *left-most* set) and subthalamic (green, *right-most* set) sites. (**B**) A scatter plot of peak NBG frequencies across sites in subject hemispheres where NBG was recorded at both sites. The dotted line indicates where the frequency would be the same at both sites, serving as a visual aid for comparing the frequencies across sites. (**C**) Contingency tables relating clinical history of dyskinesia with NBG for cortical (*left*) and subthalamic (*right*) electrode sites. Each data-point represents a subject, where each subject was classified as exhibiting NBG if one or both hemispheres had NBG oscillations exceeding the detection threshold. STN = subthalamic nucleus.

in the subject who did not meet the clinical criteria for dyskinesia (Fig. 2C). The observed patterns among the subjects suggest narrowband gamma oscillations in the motor network likely occur in subjects with a clinical history of dyskinesia, though this comparison was underpowered for formal statistical analysis. Additionally, the mean integrated gamma scores were smaller in hemispheres of subjects without a clinical history of dyskinesia than in subjects with a clinical history of dyskinesia at the cortical ($t = 2.15$, $P = 0.046$) and subthalamic ($t = 3.25$, $P = 0.007$) sites (Supplementary Fig. 2B). These results show that narrowband gamma differs between subjects as a function of the presence or absence of dyskinesia. To further investigate whether the lack of narrowband gamma in some patients with a history of dyskinesia may be due to electrode placement, we also plotted anatomic coordinates of cortical leads segregated by presence or absence of narrowband gamma, and did not find a systematic difference (Supplementary Fig. 2C).

Spectral power of narrowband gamma oscillations correlates to wearable dyskinesia scores

We examined the relationship between fluctuations in narrowband gamma power and fluctuations in continuous dyskinesia scores from the contralateral wearable device for each hemisphere of subjects with non-zero UPDRS dyskinesia preoperative scores. Examples of the narrowband gamma and dyskinesia time series are shown in Fig. 3A. Cortical narrowband gamma, subthalamic narrowband gamma and narrowband gamma coherence between the two sites correlated to the wearable dyskinesia signal (false discovery rate-corrected $P < 0.05$) in 15/17, 12/13 and 11/13 hemispheres (Fig. 3B).

Correlations between narrowband gamma oscillations and wearable dyskinesia scores yielded mean correlation coefficients of $\rho = 0.48$ for the motor cortex, $\rho = 0.53$ for the subthalamic nucleus and $\rho = 0.31$ for subthalamic-motor cortex coherence. Each correlation was significant using a one-sample *t*-test, with $P < 0.005$. The distributions differed across sites ($F = 5.11$, $P = 0.01$; Fig. 3C) and were driven by differences between coherence and cortical distributions ($F = 2.39$, $P = 0.02$) and coherence and subthalamic distributions ($F = 2.83$, $P = 0.009$). However, cortical and subthalamic distributions did not differ ($t = 0.73$, $P = 0.47$), indicating narrowband gamma oscillations at multiple sites in the motor network have similar predictive power for the occurrence of dyskinesia in a group-level analysis. Narrowband gamma fluctuations were anticorrelated with bradykinesia scores at the cortical (Supplementary Fig. 5) and subthalamic (Supplementary Fig. 6) sites. Narrowband gamma fluctuations were also anticorrelated with tremor scores but relatively less than with bradykinesia scores.

Power distribution of correlated narrowband gamma signal

Electrocorticography field potential recordings generally have a higher signal spectral power than local field potentials from subcortical structures.[12] To assess their relative spectral power in the narrowband gamma ranges, we compared the average peak narrowband gamma spectral power across the 15 cortical and 12 subthalamic sites of the subject hemispheres with correlated narrowband gamma signals and a history of clinical dyskinesia. The spectral power of the narrowband gamma oscillations was not significantly different across sites when comparing spectral power after normalization to the 1/*f* baseline ($t = 1.05$, $P = 0.30$; Fig. 3D). However, spectral power comparisons for absolute spectral power values (not normalized to baseline 1/*f*) showed a greater spectral power in the cortex, consistent with its generally higher 1/*f* baseline (Supplementary Fig. 4).

Time-lag comparison of narrowband gamma correlation distributions

To assess whether variations in narrowband gamma oscillations led or lagged the variations in dyskinesia scores, we compared correlations at various sample lags up to ±10 data-points (20 min lag time) (Fig. 3E). For the cortical narrowband gamma lag analysis, the median maximal correlation occurred at a sample lag of zero, indicating simultaneity with dyskinesia scores (within the temporal resolution of 2 min). For the subthalamic narrowband gamma lag analysis, the median maximal correlation occurred at a sample lag of −1. We assessed the significance of this apparent sample lag by comparing the distributions of sample lags at −1 with those for zero (simultaneous occurrence). The increased occurrence at a sample lag of −1 compared to zero (no lag) approached significance ($\chi^2 = 3.0$, $P = 0.08$; Fig. 3F). This indicated that fluctuations in narrowband gamma oscillations occur at the same time as, or slightly precede, fluctuations in dyskinesia scores within the 2-min resolution available in wearable scores.

Stratification analysis shows outliers do not drive correlations

Correlations can be driven by outliers, for example, when dyskinesia scores are in the bottom 10th percentile. Thus, a correlation

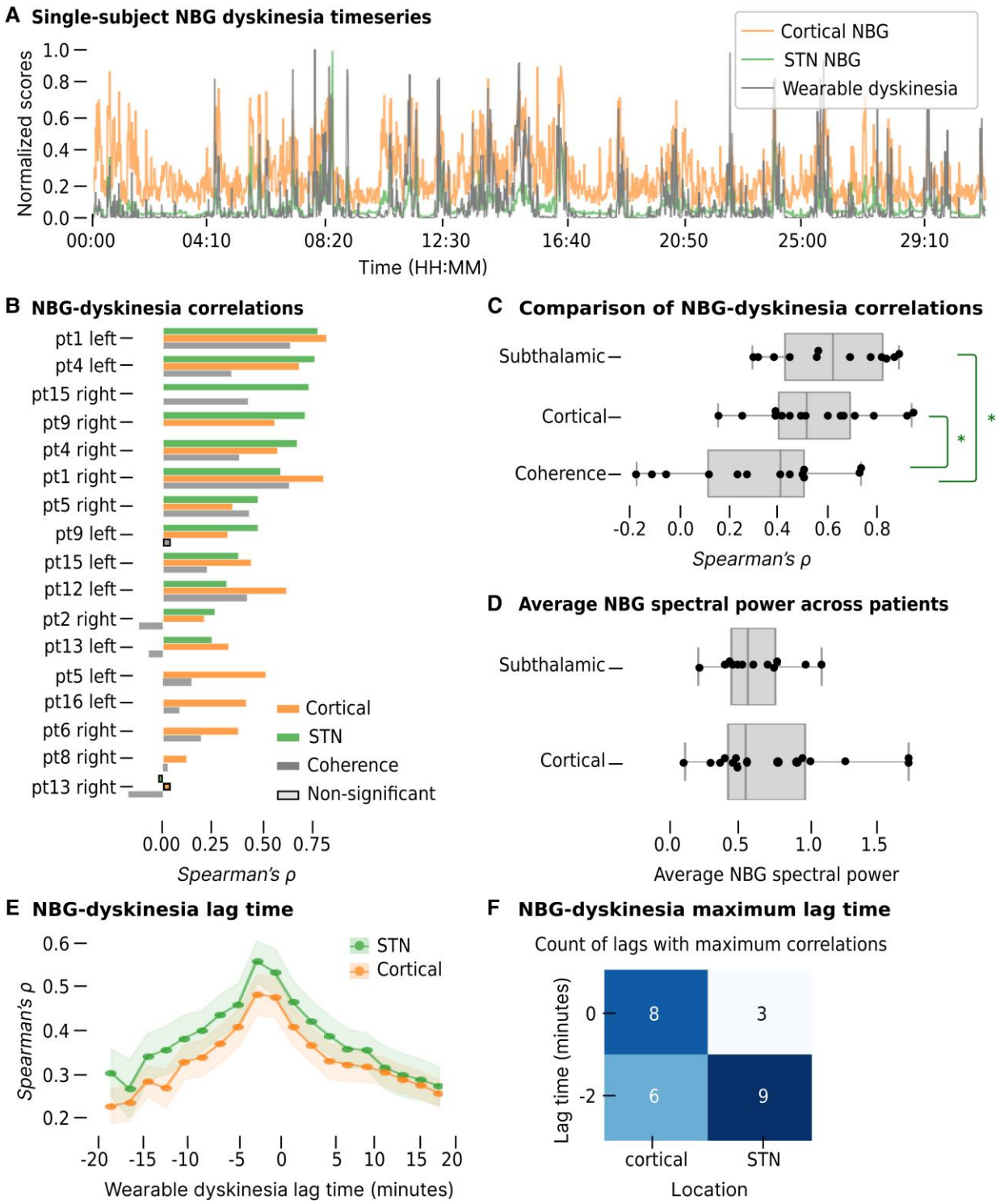

Figure 3 Narrowband gamma correlates with simultaneous contralateral wearable dyskinesia scores. (**A**) Example of a time series of power at the peak frequency of the cortical narrowband gamma (NBG, orange) and subthalamic NBG (green) in comparison with the dyskinesia scores from the contralateral wearable devices (grey, thickest line) of Subject 4's left hemisphere. (**B**) The correlations with false discovery rate-corrected $P < 0.05$ between the time series NBG signal and wearable dyskinesia scores across our subject subcohort with a clinical history of dyskinesia. Green labels (*top bars*) represent correlations from subthalamic NBG, orange labels (*middle bars*) represent correlations from cortical NBG, and grey labels (*bottom bars*) represent correlations from NBG coherence between cortical and subthalamic electrode sites. (**C**) Box plots of correlation coefficients across subject hemispheres for subthalamic NBG, cortical NBG and NBG coherence across the sites, showing higher correlation for single site spectral power than for inter-site coherence. (**D**) Box plots of the average NBG spectral power (normalized to 1/*f* baseline) across hemispheres, showing similar spectral power at cortical and subthalamic sites using an independent *t*-test. The signal spectral power also did not differ in a paired subset analysis of 10 subject hemispheres with both cortical and subthalamic NBG ($t = 1.43$, $P = 0.19$). (**E**) Pearson correlation lag analysis illustrates the strength and direction of the correlation of each lag value. The maximum correlation showed an apparent negative lag of one sample (gamma leading dyskinesia by 2 min) for subthalamic nucleus (STN, green line), but this did not meet statistical significance across subjects according to chi-square testing of categorical sample lags across subjects, shown in **F**.

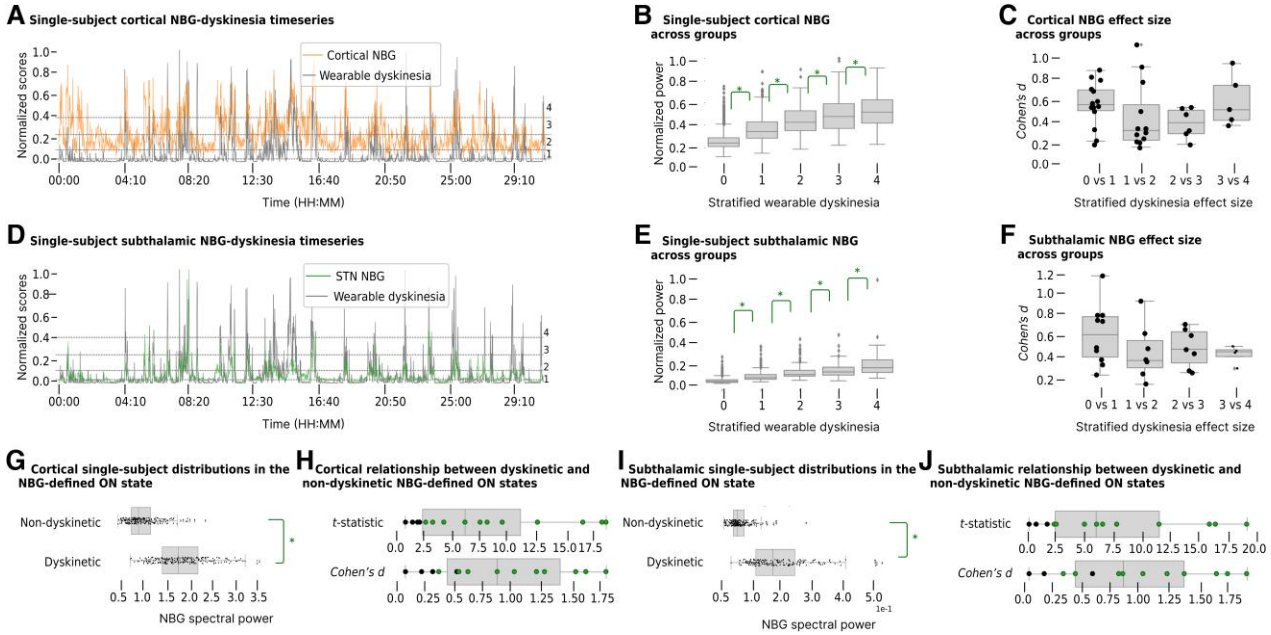

Figure 4 Stratification analysis shows narrowband gamma-dyskinesia correlations are not driven by outliers. Data are from subjects who have narrowband gamma (NBG) oscillations at the specified site, as well as a clinical history of dyskinesia. (**A**) Example time series of cortical NBG (orange) and dyskinesia scores (grey), derived from Fig. 3A but with horizontal grey dotted lines that denote the thresholds used to bin the wearable dyskinesia scores. Bins are labelled 0, 1, 2, 3 and 4. (**B**) Single-subject example (Subject 4, left hemisphere) showing the *t*-test comparison for cortical NBG between each paired, ordinal wearable dyskinesia category. (**C**) The effect size using Cohen's *d* between cortical NBG of each ordinal pair of dyskinesia categories with false discovery rate-corrected $P < 0.05$ across subjects. (**D**) Example time series of subthalamic NBG (green) and dyskinesia (grey) scores derived from Fig. 3A with the same structure as in **A**. (**E**) A single-subject example (Subject 4, left hemisphere) for subthalamic NBG, same format as in **B**. (**F**) The effect size using Cohen's *d* between subthalamic NBG of each ordinal bin with false discovery rate-corrected $P < 0.05$ across the cohort. (**G**) A single-subject example from Subject 4's left hemisphere shows the *t*-test comparison of cortical NBG between the non-dyskinetic and dyskinetic states. (**H**) The significance and effect size for cortical NBG between the dyskinetic and non-dyskinetic states across subjects, with significant data-points (false discovery rate-corrected $P < 0.05$) denoted in green. (**I**) A single-subject example (Subject 4, left hemisphere) showing the *t*-test comparison for subthalamic NBG spectral power between the non-dyskinetic and dyskinetic states. (**J**) The significance and effect size for subthalamic NBG between the dyskinetic and non-dyskinetic states across subjects, with significant data-points (false discovery rate-corrected $P < 0.05$) denoted in green. The asterisk denotes a comparison with false discovery rate-corrected $P < 0.05$. STN = subthalamic nucleus.

is insufficient to demonstrate whether narrowband gamma fluctuates as a function of dyskinesia over a wide range of severity versus indexing mainly the presence or absence of dyskinesia. To control for this possibility, we binned the continuous dyskinesia scores into ordinal bins (Fig. 4A and D, dashed horizontal lines) and compared narrowband gamma across the paired, ordinal bins in single subjects with cortical (Fig. 4B) and subthalamic (Fig. 4E) narrowband gamma oscillations. We confirmed that narrowband gamma between paired ordinal bins of dyskinesia scores differed across subjects. Differences in narrowband gamma comparisons across paired ordinal bins remained significant ($P < 0.05$) with consistent effect sizes at cortical (Fig. 4C) and subthalamic (Fig. 4F) sites. These relationships indicated that gamma-band oscillations scale with dyskinesia scores over a wide range of severity.

In the absence of neurostimulation, dyskinesias can only occur during ON-medication states, so assessing whether narrowband gamma is more predictive of the dyskinetic state compared to the ON-medication state without dyskinesia is important. First, we removed all data collected during OFF-medication states, which we defined as the top 70th percentile of bradykinesia scores within subjects. Then, we stratified narrowband gamma oscillations from the remaining ON-medication state data into three categories: non-dyskinetic (bottom 30th percentile dyskinesia scores within subjects), dyskinetic (top 30th percentile) and transitional (middle 40th percentile) at both cortical (Fig. 4G) and subthalamic (Fig. 4I) sites. Comparisons showed dyskinetic ON-states had higher narrowband gamma spectral power than non-dyskinetic ON-states in 11/17 and 10/13 subject hemispheres at cortical and subthalamic sites, respectively, with $P < 0.05$. Average *t*-statistics and Cohen's *d* values were 3.77 and 1.14 at cortical (Fig. 4H) and 4.22 and 1.12 at subthalamic (Fig. 4J) locations, respectively. Comparisons between the binned dyskinesia categories generated from the entire set of wearable scores (Fig. 4C and F) and the clinical subdomain categories (Fig. 4G and I) can be found in Supplementary Fig. 7.

Relation of narrowband gamma to normal voluntary movement

We collected wearable dyskinesia scores across our subject cohort, regardless of whether subjects had a history of dyskinesia. In two subjects without a clinical history of dyskinesia but who exhibited cortical narrowband gamma (Subject 7 left- and Subject 11 right-hemisphere), the correlation coefficients between wearable dyskinesia scores and cortical narrowband gamma were significantly positive, with $\rho = 0.02$ and $\rho = 0.16$, respectively (mean integrated narrowband gamma score of 0.036 versus 0.113 in subjects with a history of dyskinesia). This suggested that (i) the dyskinesia monitor may generate non-zero dyskinesia scores from normal voluntary movement; and (ii) narrowband gamma may also correlate with normal movement, consistent with its prokinetic function.

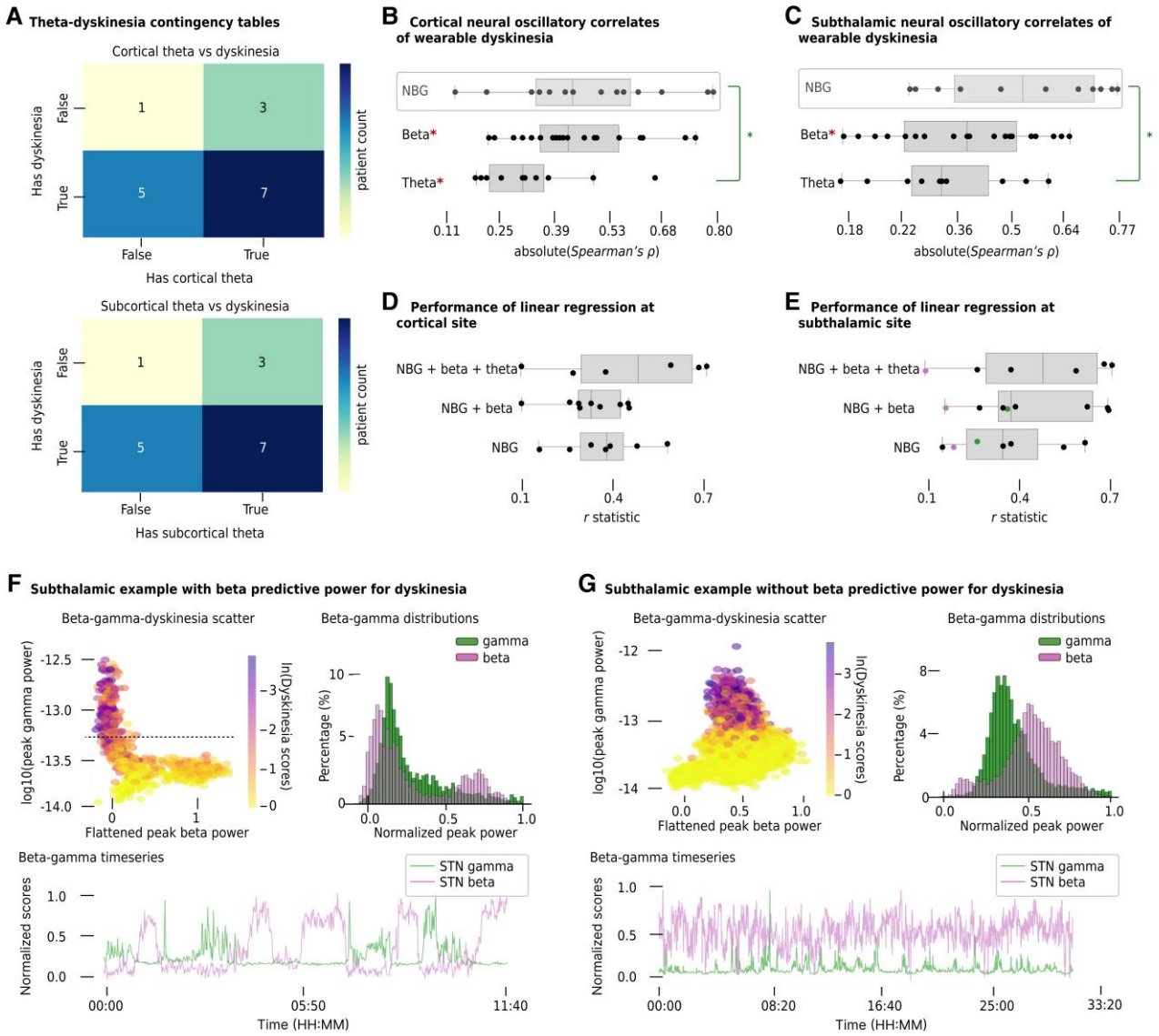

Figure 5 Other neural correlates of dyskinesia. (**A**) Contingency tables relating a clinical history of dyskinesia with the presence of theta for cortical (*top*) and subthalamic (*bottom*) electrode sites, using the same format as Fig. 2C. (**B** and **C**) For neural correlates of dyskinesia, the magnitude of the absolute correlations of dyskinesia to theta, beta and narrowband gamma (NBG) at the cortical site (**B**) and subthalamic site (**C**), where anticorrelated are denoted with a red asterisk. The distributions of correlations were compared using an independent *t*-test with $P < 0.05$ (green asterisk). (**D** and **E**) The ability to predict dyskinesia scores using linear regression models with various sets of predictors: NBG alone, the combination of NBG and beta, or the combination of all three rhythms, at the cortical site (**D**) and subthalamic site (**E**). The green and magenta dots in **E** denote data-points corresponding to subjects analysed in greater detail in the subsequent panels. (**F** and **G**) Single-subject examples of beta-gamma-dyskinesia interactions in the right subthalamic nucleus of Subject 15 (green labelled data-point in **E**), for which including beta as an independent predictor increased predictive power by 37% (**F**) and the left hemisphere of Subject 4 (magenta-labelled data-point in **E**), for which including beta did not add predictive power (**G**). *Top left*: Plot illustrates how dyskinesia scores (coloured data-points) fluctuate at a constant gamma power as a function of beta power (for example, note how dyskinesia intensity varies along the horizontal dotted line). *Top right*: Plot shows how peak beta (magenta) and gamma (green) are distributed across the time series. *Bottom*: Plot shows how beta (magenta) and gamma (green) fluctuate throughout the time series.

Relation of other frequencies to dyskinesia and use of multiple bands to predict dyskinesia

Subthalamic theta (4–10 Hz) oscillations have also been implicated in the pathophysiology of dyskinesia.[8] On the cortical level, this relationship has not been investigated, but the spectral overlap of the subthalamic 4–10 Hz activity with the mu-rhythm (8–12 Hz) that is suppressed with movement and is less modulated in Parkinson's disease may suggest an inverse relationship.[33] The majority of subjects had theta/mu oscillations ($n = 10/16$ subjects, cortical and subcortical site), regardless of a clinical history of dyskinesia ($n = 3/4$ subjects without dyskinesia, cortical and subcortical site) (Fig. 5A). We processed these theta peaks using the same methods as for narrowband gamma but with 4 Hz as the baseline spectral power and the use of flattened spectra to remove noise artifact in lower frequency bands. Then, we compared the absolute values of theta-dyskinesia and gamma-dyskinesia correlations (Fig. 5B), and found narrowband gamma was a stronger correlate than theta at the cortical (Fig. 5B) and subthalamic (Fig. 5C) sites, with $P < 0.05$.

Since subthalamic beta oscillations (13–30 Hz) are a known OFF-state neural biomarker and cortical beta oscillations are reduced by movement, we expected beta band oscillations would

anticorrelate with dyskinesia scores. Therefore, we examined the absolute value of correlations between beta oscillations (using 13 Hz as the baseline spectral power and using flattened spectra) and dyskinesia. We found the absolute correlations of narrowband gamma oscillations and dyskinesia scores were comparable at the cortical and (Fig. 5B) subthalamic (Fig. 5C) sites.

This raised the possibility that incorporating beta, theta and narrowband gamma as independent variables in a model could increase the predictive power for dyskinesia. We therefore compared the model's predictive power (r) across linear regression models with either narrowband gamma alone, the combination of narrowband gamma and beta or the combination of all three rhythms as predictors. The inclusion of additional frequencies in a linear model did not significantly improve the predictive power for dyskinesia at the cortical (Fig. 5D) or subthalamic (Fig. 5E) sites at the group level.

However, within individual subject hemispheres, there were two cortical and four subthalamic recording sites for which predictive power for dyskinesia scores increased by more than 5% when adding beta and gamma as independent variables, versus solely gamma, to the linear regression model. As a visual aid to understanding the regression results, we generated scatter plots of beta versus gamma peak frequency power for each 2-min epoch, with dyskinesia severity represented by colour intensity (Fig. 5F and G). In an example subject hemisphere for which beta band activity provided additional predictive power (Fig. 5F), one can see that for a constant level of prokinetic gamma (dotted line), the spectral power of beta influenced the occurrence of dyskinesia. The distributions of spectral power for beta and gamma oscillations are also provided (Fig. 5F and G) to show that these distributions can be either relatively continuous (gamma) or binary (beta) in nature, behaving as either 'dimmer' switches or 'binary on/off' switches, respectively.

A distinct 40–60 Hz oscillation in some subjects

We noticed a distinct oscillation at 40–60 Hz, with a relatively broad spectral peak, in three subjects. We describe these as 'low gamma oscillations' to distinguish them from the more classic narrowband 65–90 Hz oscillations and quantify their correlations with dyskinesia scores using the same methods as for narrowband gamma (Fig. 6 and Supplementary Table 1). These oscillations occurred in the cortex, subthalamic nucleus or both sites in some subjects with a clinical history of dyskinesia (Fig. 6G). Low gamma oscillations differed from classical narrowband gamma oscillations not only in their frequency distribution (Fig. 6E), spectral peak width (Fig. 6A–D) and variation in peak frequency across sites (Fig. 6F) but also in their relationship to dyskinesia scores. In contrast to the positive correlations between subthalamic low gamma power and contralateral dyskinesia scores, cortical low gamma spectral power was anticorrelated with contralateral dyskinesia scores (Fig. 6H and I). The sample lag between dyskinesia and oscillatory activity was not distinguishable from zero (no lag) (Fig. 6J and K).

Discussion

We investigated the relationship between narrowband gamma oscillations and dyskinesia in subjects with Parkinson's disease using a sensing-enabled neurostimulator in conjunction with a wearable monitor providing continuous dyskinesia scores. We analysed 984 h of neural recordings from both sensorimotor cortex and basal ganglia nuclei in 16 individuals during normal daily activities on their usual dose of dopaminergic medications prior to initiating therapeutic stimulation. Both subthalamic and cortical narrowband gamma as well as intersite coherence correlated with dyskinesia scores with a minimal time lag. However, in individual cases, one site often exhibited a greater prediction accuracy than the other.

The physiologic role of narrowband gamma oscillations

Narrowband oscillatory activity in the 40–90 Hz range is a ubiquitous feature of healthy cortical function. It has been studied extensively in rodents and nonhuman primates, though mainly in networks unrelated to motor function.[34] This activity is thought to arise from rhythmic interactions between excitatory neurons and inhibitory interneurons. Gamma band oscillations dominate in the second and third layers of the neocortex and are thought to reflect 'bottom-up' sensory input. Throughout the neocortex, gamma oscillations anticorrelate with alpha/beta oscillations, which dominate in layers five and six and are thought to reflect 'top-down' cognitive control.[35]

Narrowband gamma in the motor cortex has not been directly observed outside of disease states or disease models. Nevertheless, a potential role of motor network gamma oscillations in normal movement should be considered. The small, but significant, correlation between peak gamma spectral power and dyskinesia scores in our two subjects without a clinical history of dyskinesia can be interpreted in several ways. It is possible that the continuous dyskinesia monitors are more sensitive than the UPDRS assessment, and thus, narrowband gamma signals in these subjects indicate subclinical dyskinesia. Alternatively, the dyskinesia monitor may score some patterns of normal voluntary movement as dyskinesias. If so, narrowband gamma oscillations may be tracking voluntary movement in patients without a clinical history of dyskinesia. Consistent with this, prior studies in Parkinson's disease patients in the ON-medication state show scaling of subthalamic gamma oscillations with the velocity of normal movement during cued movement tasks.[36,37]

It is important to distinguish narrowband gamma, an oscillatory rhythm, from broadband gamma activity (sometimes referred to as 'high gamma'). Movement-related broadband gamma increases are often apparent at 50–200 Hz frequencies in the sensorimotor cortex during movement initiation.[38] They are related to local cortical activation and likely reflect asynchronous underlying spiking activity rather than a narrowband oscillatory rhythm.[39]

Models of dyskinesia genesis

The primary clinically effective therapies for Parkinson's disease, including dopaminergic medication,[2] deep brain stimulation,[6] and pallidal thermolesion,[40] all induce narrowband gamma oscillations and reduce beta oscillations at various nodes of the motor network. These observations have led to the hypothesis that in the context of Parkinson's disease, gamma and beta oscillations serve as 'prokinetic' and 'antikinetic' rhythms, respectively, and that therapeutic interventions rebalance their relative contributions to provide a more normokinetic state. Our results generally support the hypothesis that an 'excess' of narrowband gamma oscillations creates a hyperkinetic movement state[6,40] However, in some subjects (Fig. 5F), beta activity can also influence dyskinesia severity independently of gamma band activity, supporting a model in which the balance between prokinetic and antikinetic frequencies is important in dyskinesia genesis.

Whether narrowband gamma oscillations cause dyskinesia or are simply a physiological correlate is not yet clear. Many experiments have investigated narrowband gamma oscillations in the

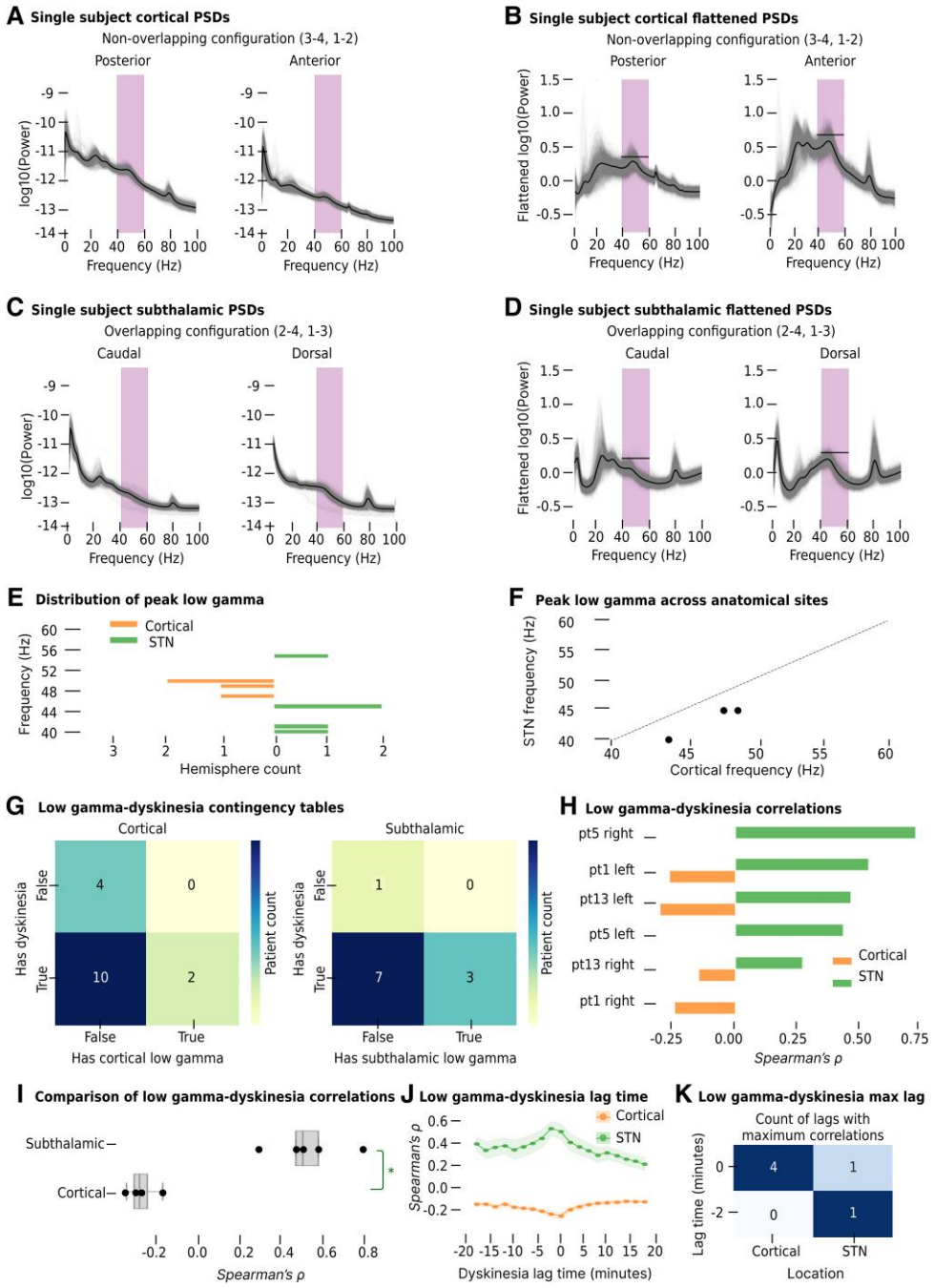

Figure 6 Low gamma processing method, frequency distribution, relation to clinical dyskinesia and correlation with contralateral dyskinesia scores. (**A**) Single-subject example (Subject 13, right hemisphere) of overlaid power spectral densities from the posterior (*left*) and anterior (*right*) recording configurations of the cortical paddle (log-scaled) during everyday life at home. Each power spectral density line (grey) is derived from a 2-min recording. The average power spectra is overlaid as the thick black line. The purple rectangle spanning 40–60 Hz denotes the signal frequencies that characterize low gamma. (**B**) Overlaid power spectral densities from **A** after removing aperiodic activity using the Fitting Oscillations and One-Over-F (FOOOF) algorithm.[13] The average flattened power spectra is overlaid as the black line. The black horizontal line is the power threshold used to detect the peak low gamma frequency. (**C**) Example of overlaid power spectral densities from the caudal (*left*) and dorsal (*right*) recording configurations of the subthalamic lead using the same format as in **A**. (**D**) Overlaid power spectral densities from **C** after removing aperiodic activity using FOOOF, similar to **B**. (**E**) The distribution of peak low gamma frequencies in cortical (orange, *left-most set*) and subthalamic (green, *right-most set*) sites. (**F**) A scatter plot of low gamma frequencies across sites in subject hemispheres where low gamma was recorded at both sites. The dotted line indicates where the frequency would be the same at both sites, serving as a visual aid for comparing the frequencies across sites. (**G**) Contingency tables relating a clinical history of dyskinesia with low gamma for cortical (*left*) and subthalamic (*right*) electrode sites. Each data-point represents a subject, where each subject was classified as exhibiting low gamma if one or both hemispheres had low gamma. (**H**) The distribution of peak low gamma frequencies in cortical (orange, *left-most set*) and subthalamic (green, *right-most set*) sites. (**I**) Box plots of correlation coefficients across subject hemispheres for subthalamic low gamma and cortical low gamma, showing that, while subthalamic low gamma positively correlated to dyskinesia scores, cortical low gamma anticorrelated to the scores. (**J**) Pearson correlation lag analysis illustrates the strength and direction of the correlation of each lag value. Dyskinesia scores are temporally shifted either prior to (positive lag scores) or after (negative lag scores) low gamma spectral power from either subthalamic (green) or cortical (orange) electrode sites. (**K**) Comparison of 0 and −2 min lag times with maximum low gamma–dyskinesia correlations across electrode sites. The asterisk denotes a comparison with $P < 0.05$ using a *t*-test, STN = subthalamic nucleus.

6-hydroxydopamine-treated rodent model of Parkinson's disease,[3-5] where experimental interventions to probe causality are more readily performed than in humans. In this model, the induction of dyskinesia by administration of levodopa or dopamine agonists was associated with the simultaneous emergence of pathological gamma-band oscillations in the cortico-basal ganglia-thalamic circuitry. The suppression of cortical gamma oscillations by administration of topical dopamine antagonists also immediately eradicated dyskinesia, suggesting a causal relationship. Nevertheless, the mechanistic link between the dopamine-depleted, levodopa-treated state and the emergence of abnormal 'prokinetic' oscillations has not been established.

Other physiological models for the generation of dyskinesia have also been proposed. Mouse optogenetic studies suggest a model that attributes dyskinesia to abnormal firing rates of specific populations of neurons in the basal ganglia, particularly within the striatum.[41,42] In this model, dyskinesia is thought to originate from the excessive activation of a subpopulation of D1-positive, direct pathway striatal neurons. A strength of the neuronal firing rate model is that it offers a specific cellular basis for dyskinesia, which can be directly manipulated using optogenetics. However, when applied to humans, models based on abnormal firing rates in the basal ganglia-thalamocortical circuit have difficulty accounting for some important clinical phenomena. Interventions that reduce activity in the internal globus pallidus, such as reversible or irreversible lesioning, suppress rather than exacerbate dyskinesia.[43] A mechanistic neural model of dyskinesia that accounts for physiological and surgical observations across species has yet to be developed.

Gamma oscillations at other frequencies are functionally distinct

The existing literature on narrowband gamma in Parkinson's disease in animal models of parkinsonism has focused on oscillatory rhythms in the 65–90 Hz range. Gamma oscillations at other frequencies are likely functionally distinct in the motor network. High-frequency oscillations at 250–350 Hz have been described in both the subthalamic nucleus and globus pallidus. Their attributes may delineate the two current motor subtypes of Parkinson's disease, tremor dominant versus postural instability with gait disorder subtypes.[44,45] These oscillations increase during voluntary movements and with dopaminergic medication, indicating their potential role in normal basal ganglia function. However, these high-frequency signals, particularly in the globus pallidus, are more pronounced in a dopamine-depleted state, unlike 65–90 Hz narrowband gamma oscillations.

Furthermore, our study revealed the presence, in some subjects, of distinct oscillations in the gamma band at lower frequencies (40–60 Hz) than the classical narrowband gamma range. These low gamma rhythms did not show functional or temporal co-occurrence with 65–90 Hz narrowband gamma oscillations. While the spectral power of 65–90 Hz narrowband gamma correlated with dyskinesia (Fig. 3B), the spectral power of cortical low gamma anticorrelated with dyskinesia (Fig. 6G). The greater bandwidth of the low gamma power spectral density peak may also hint at a different underlying physiologic mechanism.

Narrowband gamma as a marker for closed-loop deep brain stimulation

Adaptive deep brain stimulation relies on neural signals to infer the subject's clinical state and auto-adjust stimulation parameters to meet changing brain needs.[46] A prospective closed-loop marker requires that signals be sensitive and specific to the pathological state and time-locked to motor signs. The use of narrowband gamma as a control signal for adaptive deep brain stimulation with existing sensing-enabled neurostimulators has been demonstrated,[47,48] and the entrainment of gamma rhythms by therapeutic neurostimulation at a stable and predictable frequency (subharmonics of stimulation frequency) is an advantage for the use of this signal.[49] The present work supports the utility of narrowband gamma as a control signal for adaptive deep brain stimulation by showing that this rhythm correlates to symptom fluctuations across varying spectral power of dyskinesia with minimal temporal lag. Either the subthalamic nucleus or the motor cortex may serve as the site for signal detection since narrowband gamma spectral power at either site are roughly equal predictors of dyskinesia in a cross-subjects analysis. However, adaptive deep brain stimulation in Parkinson's disease may require sensing neural signals 'during' active stimulation, and stimulation artefacts will likely interfere with subthalamic sensing more than cortical sensing. Of note, theta oscillations in the subthalamic nucleus have been shown to correlate to dyskinesia.[50] We replicated this finding, but found that, unlike narrowband gamma, the relationship of theta band activity to dyskinesia was not present in the motor cortex. Furthermore, theta-alpha oscillations may be strongly affected by OFF-period tremor,[51] limiting their utility as a control signal in adaptive deep brain stimulation.

Limitations

Although the analysis of the relationship between dyskinesia scores and gamma oscillations had high statistical power within subjects due to the long duration of recordings, the cross-subject correlations were underpowered due to the relatively small number of subjects, as is typical of invasive human studies. Subjects wore wearables on the wrist; therefore, the sensor captured upper body dyskinesia rather than leg dyskinesia. Additionally, dyskinetic motor signs on the contralateral side may influence the lateralized dyskinesia scores. The proprietary algorithm generating the dyskinesia scores used was not personalized to each subject[52] and was susceptible to false positives, as voluntary movement elicits a non-zero dyskinesia score. A similar gyroscope-based heuristic algorithm to classify tremor resulted in a false positive rate of 10% when tested on healthy controls.[53] Future studies may benefit from personalized dyskinesia monitors that include lower as well as upper extremities for precise assessment.

Within the detection threshold employed here, we did not always detect narrowband gamma at cortical and subcortical sites in dyskinetic subjects. This may be due to limited spatial sampling using single quadripolar lead arrays at each site, which is a particularly important consideration for cortical recording since the precentral gyrus is both large and functionally heterogeneous.[54] Even within the motor territories of basal ganglia nuclei, electrophysiologic markers of motor signs in Parkinson's disease are known to differ in adjacent subregions.[44,55-57] Furthermore, we did not detect pallidal narrowband gamma—possibly because we were underpowered in our sample size, did not sample the relevant regions of the pallidum or because narrowband gamma was not present in the pallidum. Prior findings of strong narrowband gamma coherence between pallidum and subthalamic nucleus in the ON-medication state suggest that a larger sample of pallidal recordings might allow the detection of pallidal narrowband gamma.[2,37]

Conclusions

Narrowband gamma spectral power in the motor network (i) scales with the severity of dyskinesias; (ii) heralds dyskinesia onset without a time lag; and (iii) correlates equally with dyskinesia at both cortical and subthalamic sites. Including additional oscillatory frequencies as covariates in a predictive model of dyskinesia can increase prediction accuracy in a subset of subjects.

Data availability

Neural and wearable data can be made available upon request.

Acknowledgements

We thank David Segar for a critical manuscript review and Lauren Hammer for data analysis feedback.

Funding

Grant number: UH3NS100544, Funding body: National Institutes of Health; Grant number: R01NS090913, Funding body: **National Institutes of Health**; Grant number: U24 NS113637-01, Funding body: **National Institutes of Health**. WJN received funding for project 101077060 from the **European Research Council**, and Project-ID 424778381 – TRR 295 from the **German Research Foundation**.

Competing interests

Devices were provided at no charge by Medtronic Inc. P.A.S. and C.d.-H. are inventors on US patent # 9295838 'Methods and systems for treating neurological movement disorders'; the patent covers cortical detection of physiological biomarkers in movement disorders, which is also a topic in this manuscript. P.A.S. receives funding from Medtronic Inc. for salary support of clinical fellows.

Supplementary material

Supplementary material is available at *Brain* online.

References

1. Brown P, Williams D. Basal ganglia local field potential activity: Character and functional significance in the human. *Clin Neurophysiol*. 2005;116:2510-2519.
2. Brown P, Oliviero A, Mazzone P, Insola A, Tonali P, Di Lazzaro V. Dopamine dependency of oscillations between subthalamic nucleus and pallidum in Parkinson's disease. *J Neurosci*. 2001;21:1033-1038.
3. Güttler C, Altschüler J, Tanev K, et al. Levodopa-Induced dyskinesia are mediated by cortical gamma oscillations in experimental parkinsonism. *Mov Disord*. 2021;36:927-937.
4. Halje P, Tamtè M, Richter U, Mohammed M, Cenci MA, Petersson P. Levodopa-induced dyskinesia is strongly associated with resonant cortical oscillations. *J Neurosci*. 2012;32:16541-16551.
5. Salvadè A, D'Angelo V, Di Giovanni G, et al. Distinct roles of cortical and pallidal β and γ frequencies in hemiparkinsonian and dyskinetic rats. *Exp Neurol*. 2016;275(Pt 1):199-208.
6. Swann NC, de Hemptinne C, Miocinovic S, et al. Gamma oscillations in the hyperkinetic state detected with chronic human brain recordings in Parkinson's disease. *J Neurosci*. 2016;36:6445-6458.
7. Gilron R, Little S, Perrone R, et al. Long-term wireless streaming of neural recordings for circuit discovery and adaptive stimulation in individuals with Parkinson's disease. *Nat Biotechnol*. 2021;39:1078-1085.
8. Alonso-Frech F, Zamarbide I, Alegre M, et al. Slow oscillatory activity and levodopa-induced dyskinesias in Parkinson's disease. *Brain*. 2006;129(Pt 7):1748-1757.
9. Stanslaski S, Herron J, Chouinard T, et al. A chronically implantable neural coprocessor for investigating the treatment of neurological disorders. *IEEE Trans Biomed Circuits Syst*. 2018;12:1230-1245.
10. Follett KA, Weaver FM, Stern M, et al. Pallidal versus subthalamic deep-brain stimulation for Parkinson's disease. *N Engl J Med*. 2010;362:2077-2091.
11. Okun MS, Fernandez HH, Wu SS, et al. Cognition and mood in Parkinson's disease in subthalamic nucleus versus globus pallidus interna deep brain stimulation: The COMPARE trial. *Ann Neurol*. 2009;65:586-595.
12. Swann NC, de Hemptinne C, Miocinovic S, et al. Chronic multisite brain recordings from a totally implantable bidirectional neural interface: Experience in 5 patients with Parkinson's disease. *J Neurosurg*. 2018;128:605-616.
13. Donoghue T, Haller M, Peterson EJ, et al. Parameterizing neural power spectra into periodic and aperiodic components. *Nat Neurosci*. 2020;23:1655-1665.
14. Shahlaie K, Larson PS, Starr PA. Intraoperative computed tomography for deep brain stimulation surgery: Technique and accuracy assessment. *Neurosurgery*. 2011;68(1 Suppl Operative):114-124; discussion 124.
15. Hammer LH, Kochanski RB, Starr PA, Little S. Artifact characterization and a multipurpose template-based offline removal solution for a sensing-enabled deep brain stimulation device. *Stereotact Funct Neurosurg*. 2022;100:168-183.
16. Horn A, Li N, Dembek TA, et al. Lead-DBS v2: Towards a comprehensive pipeline for deep brain stimulation imaging. *Neuroimage*. 2019;184:293-316.
17. Davis TS, Caston RM, Philip B, et al. LeGUI: A fast and accurate graphical user interface for automated detection and anatomical localization of intracranial electrodes. *Front Neurosci*. 2021;15:769872.
18. Penny WD, Friston KJ, Ashburner JT, Kiebel SJ, Nichols TE. *Statistical parametric mapping: The analysis of functional brain images*. Elsevier; 2011.
19. Horn A, Kühn AA. Lead-DBS: A toolbox for deep brain stimulation electrode localizations and visualizations. *Neuroimage*. 2015;107:127-135.
20. Hermes D, Miller KJ, Noordmans HJ, Vansteensel MJ, Ramsey NF. Automated electrocorticographic electrode localization on individually rendered brain surfaces. *J Neurosci Methods*. 2010;185:293-298.
21. Fischl B, Sereno MI, Tootell RBH, Dale AM. High-resolution intersubject averaging and a coordinate system for the cortical surface. *Hum Brain Mapp*. 1999;8:272-284.
22. Xiao Y, Fonov V, Bériault S, et al. Multi-contrast unbiased MRI atlas of a Parkinson's disease population. *Int J Comput Assist Radiol Surg*. 2015;10:329-341.
23. Griffiths RI, Kotschet K, Arfon S, et al. Automated assessment of bradykinesia and dyskinesia in Parkinson's disease. *J Parkinsons Dis*. 2012;2:47-55.
24. Braybrook M, O'Connor S, Churchward P, Perera T, Farzanehfar P, Horne M. An ambulatory tremor score for Parkinson's disease. *J Parkinsons Dis*. 2016;6:723-731.
25. Horne MK, McGregor S, Bergquist F. An objective fluctuation score for Parkinson's disease. *PLoS One*. 2015;10:e0124522.

26. Brownlee J. *Data preparation for machine learning*. Machine Learning Mastery; 2020.
27. Chen L, Cai G, Weng H, et al. More sensitive identification for bradykinesia compared to tremors in Parkinson's disease based on Parkinson's KinetiGraph (PKG). *Front Aging Neurosci*. 2020;12:594701.
28. Sellers KK, Gilron R', Anso J, et al. Analysis-RCS-data: Open-source toolbox for the ingestion, time-alignment, and visualization of sense and stimulation data from the Medtronic summit RC+S system. *Front Hum Neurosci*. 2021;15:714256.
29. Virtanen P, Gommers R, Oliphant TE, et al. Scipy 1.0: Fundamental algorithms for scientific computing in python. *Nat Methods*. 2020;17:261-272.
30. Kotschet K, Johnson W, McGregor S, et al. Daytime sleep in Parkinson's disease measured by episodes of immobility. *Parkinsonism Relat Disord*. 2014;20:578-583.
31. Buitinck L, Louppe G, Blondel M, et al. API design for machine learning software: experiences from the scikit-learn project. arXiv [csLG]. [Preprint] https://doi.org/10.48550/arXiv.1309.0238
32. Seabold S, Perktold J. Statsmodels: Econometric and statistical modeling with Python. In: Proceedings of the 9th Python in Science Conference. 2010. doi:10.25080/Majora-92bf1922-011
33. Heida T, Poppe NR, de Vos CC, van Putten MJAM, van Vugt JPP. Event-related mu-rhythm desynchronization during movement observation is impaired in Parkinson's disease. *Clin Neurophysiol*. 2014;125:1819-1825.
34. Miller EK, Lundqvist M, Bastos AM. Working memory 2.0. *Neuron*. 2018;100:463-475.
35. Fernandez-Ruiz A, Sirota A, Lopes-Dos-Santos V, Dupret D. Over and above frequency: Gamma oscillations as units of neural circuit operations. *Neuron*. 2023;111:936-953.
36. Brücke C, Kempf F, Kupsch A, et al. Movement-related synchronization of gamma activity is lateralized in patients with dystonia. *Eur J Neurosci*. 2008;27:2322-2329.
37. Cassidy M, Mazzone P, Oliviero A, et al. Movement-related changes in synchronization in the human basal ganglia. *Brain*. 2002;125(Pt 6):1235-1246.
38. Crone NE, Miglioretti DL, Gordon B, Lesser RP. Functional mapping of human sensorimotor cortex with electrocorticographic spectral analysis. II. Event-related synchronization in the gamma band. *Brain*. 1998;121(Pt 12):2301-2315.
39. Manning JR, Jacobs J, Fried I, Kahana MJ. Broadband shifts in local field potential power spectra are correlated with single-neuron spiking in humans. *J Neurosci*. 2009;29:13613-13620.
40. de Hemptinne C, Wang DD, Miocinovic S, Chen W, Ostrem JL, Starr PA. Pallidal thermolesion unleashes gamma oscillations in the motor cortex in Parkinson's disease. *Mov Disord*. 2019;34:903-911.
41. Ryan MB, Bair-Marshall C, Nelson AB. Aberrant striatal activity in parkinsonism and levodopa-induced dyskinesia. *Cell Rep*. 2018;23:3438-3446.e5.
42. Girasole AE, Lum MY, Nathaniel D, et al. A subpopulation of striatal neurons mediates levodopa-induced dyskinesia. *Neuron*. 2018;97:787-795.e6.
43. Vitek JL, Bakay RAE, Freeman A, et al. Randomized trial of pallidotomy versus medical therapy for Parkinson's disease. *Ann Neurol*. 2003;53:558-569.
44. Telkes I, Viswanathan A, Jimenez-Shahed J, et al. Local field potentials of subthalamic nucleus contain electrophysiological footprints of motor subtypes of Parkinson's disease. *Proc Natl Acad Sci U S A*. 2018;115:E8567-E8576.
45. Johnson LA, Aman JE, Yu Y, et al. High-Frequency oscillations in the Pallidum: A pathophysiological biomarker in Parkinson's disease? *Mov Disord*. 2021;36:1332-1341.
46. Neumann WJ, Gilron R, Little S, Tinkhauser G. Adaptive deep brain stimulation: From experimental evidence toward practical implementation. *Mov Disord*. 2023;38:937-948.
47. Swann NC, de Hemptinne C, Thompson MC, et al. Adaptive deep brain stimulation for Parkinson's disease using motor cortex sensing. *J Neural Eng*. 2018;15:046006.
48. Oehrn CR, Cernera S, Hammer LH, et al. Personalized chronic adaptive deep brain stimulation outperforms conventional stimulation in Parkinson's disease. medRxiv. [Preprint] doi:10.1101/2023.08.03.23293450
49. Sermon JJ, Olaru M, Ansó J, et al. Sub-harmonic entrainment of cortical gamma oscillations to deep brain stimulation in Parkinson's disease: Model based predictions and validation in three human subjects. *Brain Stimul*. 2023;16:1412-1424.
50. di Biase L, Pecoraro PM, Carbone SP, Caminiti ML, Di Lazzaro V. Levodopa-Induced dyskinesias in Parkinson's disease: An overview on pathophysiology, clinical manifestations, therapy management strategies and future directions. *J Clin Med Res*. 2023;12:4427.
51. Contarino MF, Bour LJ, Bot M, et al. Tremor-specific neuronal oscillation pattern in dorsal subthalamic nucleus of parkinsonian patients. *Brain Stimul*. 2012;5:305-314.
52. Khodakarami H, Shokouhi N, Horne M. A method for measuring time spent in bradykinesia and dyskinesia in people with Parkinson's disease using an ambulatory monitor. *J Neuroeng Rehabil*. 2021;18:116.
53. Mahadevan N, Demanuele C, Zhang H, et al. Development of digital biomarkers for resting tremor and bradykinesia using a wrist-worn wearable device. *NPJ Digit Med*. 2020;3:5.
54. Gordon EM, Chauvin RJ, Van AN, et al. A somato-cognitive action network alternates with effector regions in motor cortex. *Nature*. 2023;617:351-359.
55. van Wijk BCM, Neumann WJ, Kroneberg D, et al. Functional connectivity maps of theta/alpha and beta coherence within the subthalamic nucleus region. *Neuroimage*. 2022;257:119320.
56. Lofredi R, Neumann WJ, Bock A, et al. Dopamine-dependent scaling of subthalamic gamma bursts with movement velocity in patients with Parkinson's disease. *Elife*. 2018;7:e31895.
57. Horn A, Neumann WJ, Degen K, Schneider GH, Kühn AA. Toward an electrophysiological "sweet spot" for deep brain stimulation in the subthalamic nucleus. *Hum Brain Mapp*. 2017;38:3377-3390.